ACS OMEGA

Article

Cite This: ACS Omega 2020, 5, 170−178

http://pubs.acs.org/journal/acsodf

Computational Analysis of the Silver Nanoparticle−Human Serum Albumin Complex

Zaved Hazarika and Anupam Nath Jha*

Computational Biophysics Laboratory, Department of Molecular Biology and Biotechnology, Tezpur University, Tezpur 784028, Assam, India

Supporting Information

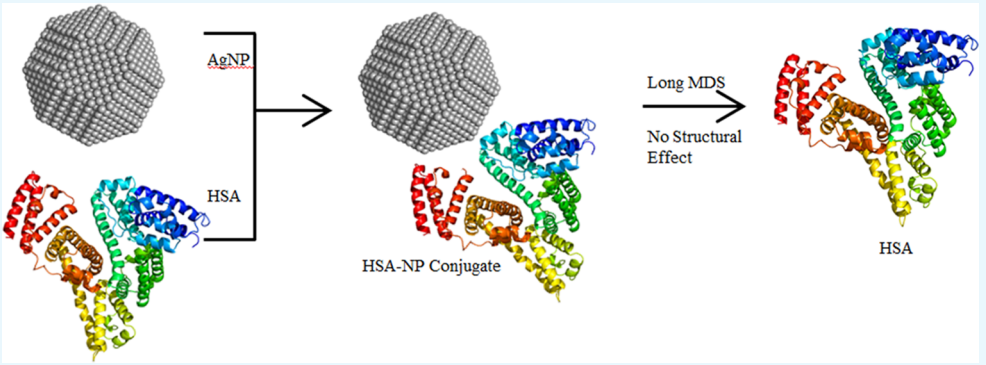

ABSTRACT: Drug delivery in excess concentrations and at not-specified sites inside the human body adversely affects the body and gives rise to other diseases. Several methods have been developed to deliver the drugs in required amounts and at specific targets. Nanoparticle-mediated drug delivery is one such approach and has gained success at primary levels. The effect of nanoparticles on the human body needs important apprehension, and it has been unraveled by assessing the protein−nanoparticle interactions. Here, we have measured the impact of silver nanoparticles (AgNPs) on the human serum albumin (HSA) structure and function with the help of all-atom molecular dynamics simulations (MDS). HSA is a transport protein, and any change in the structure may obstruct its function. The post MD analyses showed that the NP interacts with HSA and the conjugated system got stabilized with time evolution of trajectories. The present investigation confirms that the AgNP interacts with HSA without affecting its tertiary and secondary structures and in turn the protein function as well. AgNP application is recommended in transporting conjugated drug molecules as it has no adverse effect on serum proteins. Since HSA is present in the circulatory system, it may open various applications of AgNPs in the biomedical field.

1. INTRODUCTION

Nanoparticles (NPs) are materials of sizes in the range of nanometers (1−100 nm), and they possess different physical, optical, and electronic properties compared to those of their bulk counterparts.[1] NPs exhibit different properties due to their sizes and high surface areas compared to bulk materials and have various applications in diverse fields. Neamtu et al. used functionalized magnetic nanoparticles for wastewater treatment.[2] Nanoparticles have been used in hydrogen sensors,[3] photoacoustic molecular imaging,[4] solar cells,[5] and chemical products such as cosmetics, polymer fillers, catalysts, and many more.[6]

NPs have various biomedical applications such as in bioimaging,[7,8] diagnosis,[9,10] and drug delivery.[11] There are mainly two approaches that have been used in drug delivery. One is the conjugation of drugs with a suitable nanoparticle to deliver at the site of action, and another is to encapsulate the drug inside a nanoparticle for subsequent release at the specific cell or tissue. These approaches depend upon the type of nanoparticle as well as the ligand property and have advantage over traditional drug delivery. In this method, lesser amounts of the drug are needed to be administered into the body, which also reduce the unwanted side effects.[12,13]

Nanoparticles upon coming in contact with biomolecules (e.g., proteins, DNA, or lipids) interact with each one of them in a specific manner.[14] Proteins form a layer around NPs, which is termed as protein corona after having an interaction with the nanoparticle. The biological reactivity of the different nanoparticles is dictated by the stability of the protein corona. In the recent times, different types of research have been done on the protein−nanoparticle aspect, which aid in understanding the adsorption behavior of NPs on proteins.[15] The adsorption of the protein onto the nanoparticle may bring some conformational rearrangement, which might alter the protein function. Apart from the adsorption pattern, studies focus on the effect of nanoparticles on the three-dimensional

Received: July 25, 2019
Accepted: November 7, 2019
Published: December 24, 2019

DOI: 10.1021/acsomega.9b02340
ACS Omega 2020, 5, 170−178

structure of the protein.[16] Factors contributing to conformational changes in the proteins are shape, size, surface charge, and the type of nanoparticles. As the function depends upon the 3D structure of the protein, significant changes in the structure shall lead to inactivity of the protein, which in turn makes it toxic. Ahmed et al. screened fullerene-based nanoparticles on varied protein targets encompassing different biological functions.[17]

Different groups have used various types of nanomaterials to study their effects on biomolecules. Investigations using both experimental and computational approaches give insight into the protein−NP interactions at the molecular level. Experimental studies provide understanding at the macroscopic level, for example, Chatterjee et al. showed the structural changes of the ToxR protein of *Vibrio cholerae* upon ZnO NP binding.[18] Computational approaches based on molecular dynamics simulations (MDS) and density functional theory assist in understanding the protein−NP interactions at the atomic level, for example, Radic et al. delineated the role of the surface chemistry of fullerene on protein misfolding, and also Tang et al. showed unfolding of collagen triple helices with gold NPs.[19,20] Luan et al. also showed the toxicity of graphene sheets by MDS.[21] Combination of experimental and computational techniques has been used to analyze the efficacy of antimicrobial peptides (nisin) upon conjugation with silver nanoparticles (AgNPs).[22]

Earlier work from our group has helped us to understand the applicability of the drug delivery property of CNTs (carbon nanotubes) mediated by fullerenes as a function of time.[23] Also, we have shown how graphene, SWCNTs (single-wall carbon nanotubes), and boron nitride nanomaterials facilitate and improve the recognition of pyrazinamide drug molecules in the active site of the pncA protein.[24,25] The effect of moonlight protein bovine lactoferrin (BLF) and AgNP conjugation on protein conformation, NP cytotoxicity, and its bacteriostatic function was analyzed.[15] Interaction of insulin with ZnO NPs has led to enhanced rates of its fibrillation wherein ZnO NPs act as a favorable template for insulin nucleation and growth, which ultimately leads to amyloid fibril formation.[26]

It is well understood that any drug has to transverse thorough the blood plasma to reach tissues and organs. NPs to be used for drug delivery have to come in contact with blood and interact with the most amply available blood proteins. One of the most abundant proteins in the blood system is serum albumin, which constitutes approximately 60% of the blood plasma. Fanali et al. did a comparative analysis of the serum albumins to show that, among the sequences from 49 varied organisms encompassing mammals, birds, reptiles, amphibians, and fishes, most of them are made up of three repeated domains whereas lamprey serum albumin is made up of seven domains.[27] Li et al. further did a comparative analysis of serum albumins, which includes animals, plants, bacteria, fungi, and archaea, and pointed out that serum albumins are only present in vertebrates.[28] They showed that serum albumin, α-fetoprotein, vitamin D-binding protein, and afamin had an evolutionary relationship among them and reported a new member of the albumin family termed extracellular matrix protein 1.

Human serum albumin (HSA) plays an important role in the transportation of endogenous and exogenous compounds such as fatty acids, bile acids, and a wide range of drugs. Further, HSA helps in regulating the colloid oncotic pressure.[29] Numerous studies on HSA had culminated into more than a hundred crystallographic solved structures in the protein data bank (PDB)[30] in the recent time. The culmination of so many structures can be attributed to the property of HSA, which is able to bind and transport a number of different ligands. Due to its transport function, several groups have studied the interactions of clinically important drugs and small molecules with HSA.[31,32] It had a tremendous impact on the clinical studies and led to a better understanding of the pharmacokinetics of drugs such as axitinib[33] and doxorubicin.[34]

The use of NPs in drug delivery will be feasible only when HSA−NP interaction does not change the protein conformation. It becomes important to study the effect of different NPs on the HSA structure. Ramezani et al. showed the decrement in the structural content of the HSA protein in the presence of cubic and spherical gold nanoparticles using MDS.[35] Using computational approaches, Shao and Hall brought forth another interesting aspect about the allosteric effect of HSA and prompted the community dealing with nanobiotechnology to consider it while designing and applying for biomedical purposes.[36] Leonis et al. showed interactive study of HSA with fullerenes using computational approaches.[37]

We have considered AgNPs because they are one of the most extensively investigated nanoparticles due to their therapeutic, electrical, and optical potential. They have great implications in the biomedical arena because of their antimicrobial activity;[38] also, they are used in nanosilver-based biomedical products, for example, drug-delivery platforms, orthopedic materials, and bandages, and in antimicrobial compositions.[39] Even though they have shown great potential in the ever growing field of nanobiotechnology, some adverse effects have also been reported.[40,41]

In this work, we have investigated the structural flexibility and dynamics of the HSA protein in the presence of AgNPs in different orientations, which have been considered in such a way that each domain of HSA interacts with the AgNP. In case a selected NP undergoes clinical trials in different organisms, the serum albumin from other species should also have no effect. Hence, it becomes imperative to calculate the similarity between serum albumin from humans and other species at sequence levels. The interactions between AgNP and the HSA protein have been deciphered by all-atom molecular dynamics simulation.

2. RESULTS

2.1. Sequence Analysis. Thirteen sequences of serum albumin from different organisms, including humans, after performing BLASTP were retrieved, and multiple sequence alignment (MSA) was done. The selected organisms are generally used for in vivo experiments in clinical trials. As the sequences (S1 to S13) are for the same protein, we can observe a higher amount of similarity between them (Figure S1). The maximum and minimum lengths among all the sequences are 615 (chicken) and 600 (macaque). Table 1 shows the percent identity and the query coverage of all of the sequences compared to the HSA sequence. From Table 1, we can observe that the macaque showed a maximum percent identity of 93.5% and the chicken showed a minimum percent identity of 47.45% with HSA, and the query coverage is in the range of 98−100%. Six different subdomains (present in humans) are shown in Figure S1a−f. Figure S1 shows that all of the higher organisms share a significant amount of similarity at the

DOI: 10.1021/acsomega.9b02340
ACS Omega 2020, 5, 170−178

Table 1. Sequence Identity and Query Coverage of HSA against Other Organism Sequences

seq no.	organism	UniProt ID	identity (in %)	query coverage (in %)	sequence length
S1	chicken	P19121	47.45	100	615
S2	rat	P02770	73.36	99	608
S3	mouse	P07724	72.37	99	608
S4	guinea pig	Q6WDN9	73.03	99	608
S5	rabbit	P49065	75.33	99	608
S6	pig	P08835	76.11	99	607
S7	cattle	P02769	76.61	99	607
S8	sheep	P14639	75.78	99	607
S9	horse	P35747	76.94	99	607
S10	human	P02768	100	100	609
S11	macaque	Q28522	93.50	98	600
S12	cat	P49064	82.24	98	608
S13	dog	P49822	80.26	99	608

domain level, which in turn may give them a similar 3D structure.

2.2. Simulation Trajectory Analysis. To gain insight into the dynamics of human serum albumin (HSA) with silver nanoparticles (AgNPs), we have performed MD simulations on the native protein and protein−NP complex. In order to measure the effect of AgNP on the protein's structure, we have carried out five sets of simulations wherein the AgNP spanned different domains of the protein. Information about the structural deviations and stability of the protein is provided by the parameter root-mean-square deviations (RMSDs). Figure 1a shows the RMSD plot of the protein for all the

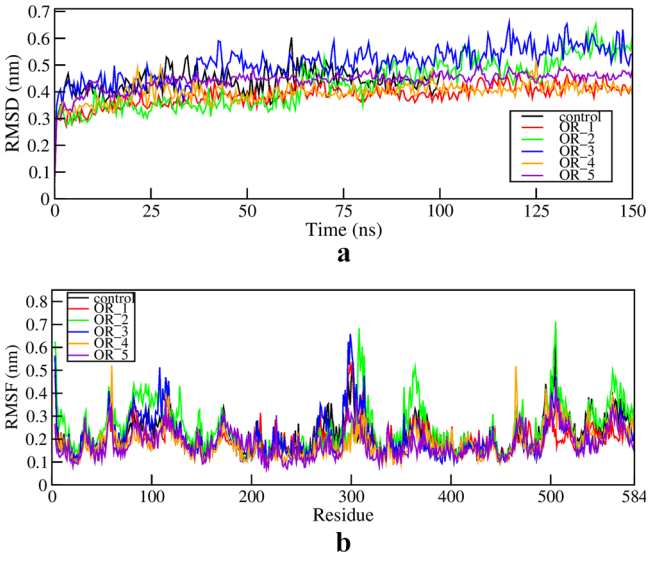

Figure 1. a: RMSD plot of HSA in the presence and absence of AgNPs. b: RMSF plot of overall fluctuations of the residues of HSA in the presence of AgNPs.

considered simulations, and from the RMSD analysis, it can be interpreted that the protein in water fluctuates in the range of 0.2 to 0.6 nm, which is similar to earlier reported simulation studies.[42,43] In the case of the control (only protein), some fluctuations are observed till 60 ns of simulation, and thereafter it gets stabilized till the end of the simulation time.

In the case of OR1, after a few fluctuations till 50 ns of time, the RMSD converges and maintains its stability until 150 ns. In OR2, the protein showed a similar behavior to that of the native structure and with few numbers of fluctuations; it converges after 130 ns. Compared to the native, OR3 showed quite a number of minor fluctuations, which stabilize toward the end of simulation, whereas in OR4 and OR5, the protein showed a similar behavior to the native. Overall, the RMSDs of the simulations in the presence of NPs were within the range of 0.3−0.6 nm. No significant changes were observed among the simulation trajectories in the presence of NPs compared to the bare protein. Additionally, the RMSD of domain regions interacting with the AgNP was observed, shown in Figure S2, which also showed a similar behavior to that of the overall RMSD analysis. Thus, the protein does not illustrate any abnormal structural change in the presence of AgNPs during complete simulation.

In order to understand the residue-wise fluctuations of the protein over the simulation time, root-mean-square fluctuations (RMSF) were calculated. The RMSF analysis sheds light on the fluctuations of residues, which in turn show their significance as any drastic changes in the flexibility of the functionally important residues will affect the HSA's function. From Figure 1b, we can observe that the overall fluctuations of the residues of the HSA in the presence of AgNPs in all five simulations were similar to those of the control. The overlap of the RMSF plots (five orientations) with that of the bare protein suggests that there is no influence on the residue flexibility of HSA upon AgNP binding.

2.3. Effect of AgNP on Individual Residues. In order to get a better picture of the behavior of the residue fluctuations, we have compared the residue level variations in the presence and absence of NPs by calculating the parameter $\Delta RMSF_i$. Comparative flexibilities of the protein residues in the presence of the NP in the five orientations are tabulated in Table 2. As

Table 2. Percentage of Residues in the Three Categories

	amino acids (in %)		
systems	<−0.4	[−0.4, 0.4]	>0.4
OR1	13	86	1
OR2	2	91	7
OR3	9	90	1
OR4	15	84	1
OR5	20	79	1

HSA is a large protein, we have considered three groups of amino acids on the basis of the numerical value of ΔRMSF. This parameter measures the relative flexibility of the residue and groups them into three categories: (i) reduced, (ii) unchanged, or (iii) increased flexibility in the presence of NPs.

From Table 2, we can observe that the flexibility of the residues follows a similar trend among the first four conjugates. In the first four conjugates, the majority of the residues fall within the unchanged category, which suggests that the presence of AgNPs does not alter their flexibility; thus, it would not affect the function rendered altogether by the protein. In OR5, in the presence of two NPs, 20% of the residue's flexibility is reduced although 79% falls in the unchanged category. Thus, it can be said that, in the presence of higher concentrations of NPs, the flexibility of residues might slightly change compared to single-NP conjugates. As the flexibility of the majority of the residues did not change, we can infer that the presence of AgNPs does not have any structural effect on the HSA protein.

DOI: 10.1021/acsomega.9b02340
ACS Omega 2020, 5, 170−178

2.4. Secondary Structure Analysis of HSA. The adsorption of any nanoparticle on the protein's surface might have an effect on the secondary structure of the protein. The function of a protein solely depends on the structure of the protein; therefore, any alteration in its structure might disrupt its normal functioning. We have carried out DSSP analysis of HSA for all of the orientations and compared it with the control. The probability values in terms of the persistence of helical and loop structural contents throughout the simulation period for all the orientations were plotted and are shown in Figure S3. From the plot (Figure S3a,b), it was inferred that the p value is more than 0.7 for most of the residues, which means that they remain in the same category of secondary structure during the simulation. Further, no noticeable variation was witnessed compared to the control, which suggests that the protein retains its structure in the presence of the NP.

To gain more insight, we have calculated the parameter ΔSec_i, which provides a comparative change in the secondary structure of individual amino acid. We have allocated the number of residues into three categories: residues that maintained their structure ($\Delta Sec_i < 0.2$), those that have moderate changes ($0.2 \leq \Delta Sec_i \geq 0.5$), and ones that changed their structure significantly ($\Delta Sec_i > 0.5$). The number of residues in these categories has been tabulated in Table 3.

Table 3. Number of Residues Categorized into Three Groups

	number of residues		
orientation	[<0.2]	[0.2, 0.5]	[>0.5]
OR1	526	50	6
OR2	539	41	2
OR3	540	42	0
OR4	543	38	1
OR5	528	50	4

Table 3 shows that approximately 95% of residues maintain their structure upon AgNP adsorption with residues mainly belonging to the helical part of the protein. Only 6−8% of the residues show moderate changes in the structure. As few residues fall into the third category, this indicates that hardly any residues show change in the secondary structure in any of the orientations. This analysis further confirms our previous observations from RMSD and RMSF analyses in that adsorption of AgNPs on the HSA protein has no negative impact on its structure.

2.5. Number of Nonbonded Contacts. From the above observations, it can be said that the selected NP makes no impact on the protein structure. Even the residue-level comparison between the simulations of bare protein and protein−NP conjugates validates that the protein remains unaltered. It may be possible that the nanoparticle is not able to interact with the protein. This possibility has been ruled out by tracking down the interaction between the AgNP and protein through the number of nonbonded contacts during the simulation. The measured number of nonbonded contacts between the nanoparticle and protein for all the orientations through the simulation time is shown in Figure 2. It can be observed in Figure 2 that all of the conjugates make a number of contacts within 6 Å, which increase at the start and are maintained till the end of simulation. Among all the conjugates, OR1 made the most nonbonded contacts followed

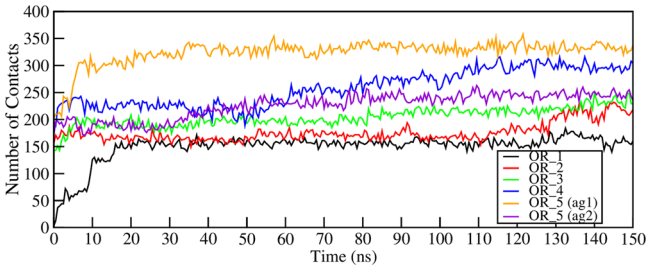

Figure 2. Number of nonbonded contacts between HSA and AgNP within 6 Å.

by OR4 and OR5 (the number of contacts for two NPs were measured separately for OR5) with AgNPs. The interactive amino acids with the AgNP have been accounted and are given in Table S1. The number of amino acids within the nonbonded distance cutoff is in the range of 18−32 in different orientations. It comprises mainly charged amino acids, which have been further validated in interaction energy calculation wherein the Coulombic energy is observed to be a highly contributing term toward the stability of the HSA−AgNP system. It can be inferred from these nonbonded interaction calculations that the protein interacts with the AgNP, and the convergence of the curves in all cases suggests that they maintain their level of interaction throughout the 150 ns time.

2.6. Protein−AgNP Interaction Energy. Additionally, the protein−NP interaction energy, which deciphers the interaction of this protein with silver nanoparticles, was quantified and compared. The process of adsorption of the AgNP on HSA in different simulations was compared on the basis of the average energy of the systems. The negative value of change in the average energy (ΔE) indicates interactions between the protein and AgNP (given in Table 4). From the data (Table 4), we can observe that the Coulombic (SR) energy is the most contributing nonbonded term toward the stable interactions between the protein and AgNP.

On comparing the ΔE of all the orientations, it was observed that OR5 is the most stable among all of the systems. It can be attributed to the fact that the fifth case consists of two NPs around the HSA protein. The interactions happening at the interphase of the HSA protein and the AgNP contribute toward the net negative energy values of the total and potential energies as shown in Table 4. This negative ΔE further confirms our nonbonded contact analysis signifying interactions happening between the AgNP and protein.

3. DISCUSSION

Use of nanoparticles in the targeted drug delivery regime is gaining importance because of their ability to hold and carry along with a slow and effective release of small molecules at the specialized locations.[9] In this process, the NP has to interact with the biomolecules, especially the proteins inside the cell. A set of nanoparticles, such as fullerene, iron oxide, silver, gold, and silica, have been tested against different proteins to see their effect on the protein structure and function.[37,44−47] In case a selected NP changes the protein structure and in turn its function, it becomes toxic and so cannot be used for drug delivery.[18] The drug-carrier nanoparticles have to interact with blood plasma proteins during the transport of molecules.

Here, we have chosen a blood plasma protein (serum albumin) to testify the use of nanoparticles as drug carriers. The NP shall carry the drug through the blood system to the

DOI: 10.1021/acsomega.9b02340
ACS Omega 2020, 5, 170−178

Table 4. Interaction Energy of the Five Simulated Systems

	ΔE (10^6 kJ mol^{-1})				
energy term	OR1	OR2	OR3	OR4	OR5
Coulombic (SR)	−2.1034	−2.4218	−1.8121	−1.8467	−3.4194
potential energy	−1.7897	−2.0522	−1.5329	−1.5627	−3.4544
total energy	−1.4670	−1.6823	−1.2563	−1.2807	−2.9176

intended target, and it becomes imperative to measure its impact on the serum albumin protein. Earlier work by Shao et al. reported the effect of gold nanoparticles on HSA and showed the changes in the secondary structure at the amino acid residue level.[36] This promoted us to select another well-studied NP, that is, the silver nanoparticle, and to measure its impact on HSA. This computational study gave an insight into the dynamics of AgNP adsorption on HSA. We have endeavored to look into the protein−NP interaction at the atomic level by using an all-atom molecular dynamics simulation technique. In experiments, multiple NPs may interact with a single protein molecule, but it is computationally expensive to introduce a number of nanoparticles in one simulation box along with the protein.[15,26] Thus, to save our computational cost and also to consider all feasible interactions, we have considered five different possible orientations of the AgNP around the HSA protein. In the all-atom explicit simulations, we have further considered AgNPs of an optimum size of 4.5 nm.[22] Too small-sized nanoparticles might get stuck in the protein binding pockets, or a NP of a bigger size may not be able to come in close contact with amino acid residues of the protein as we have considered only a single protein molecule in simulations.

As any drug or nanomedicine has to pass through the clinical phase trials,[48] we intend to take into consideration the sequence identity of albumin among such organisms, which are utilized for in vivo experiments. From the multiple sequence alignment, it can be observed that the HSA showed significant sequence identity with the other organisms, the AgNP conjugation with albumin of these organisms may provide similar outcomes.

The effect of silver nanoparticles on the HSA protein structure was measured by several simulation trajectory-based analyses. It was observed that all of the simulations with NPs have similar RMSDs to those of the control simulation suggesting that no change in the protein's structure occurred. The domain, close to NPs in different orientations, RMSD analysis also did not show any major fluctuations. The residue-level fluctuation-based changes have been accounted by RMSF analysis, which also showed similar behavior in the presence of AgNPs to that of bare protein. These results have been further verified by evaluating the parameter $\Delta RMSF_i$, which compares the residue-level changes in the presence and absence of NPs during simulations. Here, we have used only side-chain atoms to calculate the changes because they play a major role in all of the functional interactions. This analysis confirms that the protein structure remains intact even at the level of individual amino acids.

Any change in the secondary structure of the HSA protein may lead to aggregation, which in turn gives toxicity. The DSSP analysis does not show any deterioration in the secondary structure in the presence of the AgNP. We have again re-verified the changes in secondary structure at the amino acid level by comparing the score of the individual residue in protein−NP conjugate and only-protein simulations. These sets of investigations of protein−NP complexes point out that the silver nanoparticle has no negative impact on HSA.

It may be possible that the nanoparticle is not able to interact with serum proteins during the simulation time. The protein−NP interaction was tested by measuring the change in the number of nonbonded contacts and average energy values of systems over the simulation time analysis. In both analyses, we have shown that the silver nanoparticle remains in the periphery of the serum protein and the protein−NP conjugate becomes more stable with time. It is important to mention here that the nanoparticle should not have any negative effect on the biomolecules for any biomedical applications. Through an extensive MDS for multiple interactive orientations of protein−NP complexes, we have shown that the silver nanoparticle has no toxic effect on human serum albumin, which may be confirmed experimentally. These results support the use of silver nanoparticles in biomedical applications.

4. CONCLUSIONS

The effect of nanoparticles inside the human body should be checked before using them for targeted drug delivery. Experimental as well as theoretical testing of various NPs has ruled out the possibilities of their utilization for biomedical purposes because of their toxic effects on biomolecules. The interactions between biological or nanobio systems at the atomistic level can be understood by using a state-of-the-art computational technique known as molecular dynamics simulations. This theoretical work has contributed to finding the relevant and possible structural effect of AgNPs on human serum proteins.

It is important for the use of any nanomaterial that the presence of NPs should not alter the 3D structure of the protein as its function depends on its structure. Thus, with the help of extensive MD simulations, approximately 1.5 μs, we accounted no negative impact of AgNPs (4.5 nm) on the HSA protein. The structural analyses, RMSD, RMSF, and secondary structure of the protein, in the presence of the silver nanoparticle confirm that HSA behaves in a similar way to that in the absence of NPs during the complete 150 ns of dynamics. Further, the nonbonded contacts, number of interacting amino acids, and comparative analysis of energy components between proteins and nanoparticles have been measured to ensure their interactions throughout the simulation time of 150 ns. It is confirmed that the silver nanoparticle interacts with human serum albumin without affecting its tertiary and secondary structure. We believe that the AgNP has no toxic effect on the HSA protein, and it may be utilized to transport drug molecules conjugated with it.

5. METHODOLOGY

5.1. Sequence Analysis. A nanoparticle as a drug carrier can be used only if it passes through the different phases of clinical trials. NPs conjugated to a drug interact with blood plasma proteins during transportation of molecules. The structures of serum albumin (an important plasma protein)

DOI: 10.1021/acsomega.9b02340
ACS Omega 2020, 5, 170−178

of other organisms, which are used in clinical trials, should not get affected by AgNP because the altered structure may change the protein function. It may be possible only if the sequences of serum albumins from other organisms are very much similar to HSA. We have performed BLASTP[49] analysis using the input sequence of HSA (UniProt ID: P02768)[50] to find out the available similar albumins in other organisms. A total of 12 sequences similar to those of HSA were selected, and a multiple sequence alignment (MSA) was performed using Clustal Omega.[51]

5.2. System Preparation. More than 100 HSA structures are available in the RCSB Protein Data Bank.[30] We have selected a structure (PDB ID: 5ID7)[52] on the basis of resolution, the number of missing residues, and the *R* factor out of 105 human serum albumin structures, and its coordinates were retrieved from RCSB Protein Data Bank. It is a heart-shaped protein made up of 585 residues. The crystal structure of HSA has three missing residues: 1, 2, and 585. The protein is a monomer, which comprises three domains named I, II, and III. The three domains are further subdivided into two subdomains, namely, IA and IB, IIA and IIB, and IIIA and IIIB. There are two main binding sites, which are termed as Sudlow sites.[53] The first binding site is located at the core of the subdomain IIA, and the second Sudlow site is at IIIA. Apart from the Sudlow sites, there are five small pockets with the ability to bind fatty acids. As there are no missing residues in either of the Sudlow sites, we proceeded with the pdb structure. It contains 83 positively and 97 negatively charged residues. These residues are dispersed throughout the structure of the protein. It belongs to the α class of proteins having 74% amino acids in its helical structure forming, in total, 32 helices.

The nanoparticle used in this study is the silver nanoparticle (AgNP). The spherical structure of the AgNP has a diameter of 4.5 nm, taken from an earlier study.[54] The AgNP structure is made up of 3871 Ag atoms. The Lennard-Jones parameters for the AgNP were considered from the Heinz group.[55]

The AgNP and protein conjugates were prepared with the molecular modeling system Chimera.[56] We have considered five different orientations of the protein to interact with the NP (Figure S4). As mentioned above, the HSA protein has multiple active sites spread in three domains, and each of them has been reported to carry different drug molecules. The AgNP was placed near the active sites of individual domains to observe the effect of NPs on protein conformation. Only one NP was considered in the first four orientations, and two nanoparticles of the same size were used in the last conjugate. The orientations are considered such that the AgNP encompasses all the domains of the protein (Table 5). In all of the protein−NP conjugates, the exterior atoms of the NP were kept in a range of 2−4 Å from the protein's surface. The coordinates of the five orientations of the HSA protein−AgNP conjugates were further used to carry out dynamic simulations.

Table 5. NP-Facing Domain of the Protein in Different Orientations

orientation	protein domain	residue no.
OR1	III	384−582
OR2	I	5−196
OR3	IIA	197−297
OR4	IIB	298−383
OR5 (two AgNP)	IIA and IIB	197−383

5.3. Molecular Dynamics Simulations. To comprehend the functionality and dynamics of the protein and protein−ligand systems, MDS has been extensively utilized.[57−60] Therefore, in order to understand the dynamic behavior of the protein in the presence of NPs, molecular dynamics simulations were carried out with the GROMACS (Groningen Machine for Chemical Simulations) 2016.4 version.[61,62] The parameterized GROMOS 54A7 force field was utilized for all of the simulations. In this study, seven sets of simulations were carried out, that is, that of only the HSA protein and of the AgNP and five sets of protein−NP conjugate systems. All of the systems were solvated with the SPC (simple point charge) water model, which were placed in a cubic box that extends to 1.0 nm from the molecule to the edge of the box. All bonds were constrained with LINCS algorithm.[63] Periodic boundary conditions were applied in all directions. To neutralize the systems having a net negative charge of 14, prior to the dynamic run, 14 Na^+ ions were added to the protein in all simulations. This initial preparation was followed by energy minimization with the steepest descent algorithm at a tolerance of 1000 kJ mol^{-1} nm^{-1}. The minimized systems were equilibrated in two phases. First, the systems were equilibrated at constant volume and temperature (*NVT*) for 2 ns, which was then followed by a 5 ns equilibration at constant pressure and temperature (*NPT*). The temperature and pressure were fixed at 300 K and 1 bar, respectively, with the aid of a velocity-rescale thermostat[64] and Parrinello−Rahman barostat algorithm.[65] Final production runs were carried out after the equilibration phase for 150 ns with a time step of 2 fs. The number of atoms in these simulations is approximately 0.3−0.4 million. All of the trajectories of the completed production runs were analyzed with the available tools of the GROMACS package. Approximately 1.5 μs of simulation was done with a GPU-based server containing eight physical Intel Xeon CPU cores with two NVIDIA Tesla P100 graphic cards. It took an average time of 15 days to run a simulation for only one configuration. The observations were rechecked after performing repeat simulations of 100 ns for each orientation, which show similar results. Results are shown for the 150 ns runs, and the repeat simulations data are presented in the Supporting Information.

5.4. Effect of AgNP on Individual Residues. The protein structure flexibility in the presence of nanoparticles may affect the drug binding ability of serum albumin. Flexibility is an intrinsic property of molecules, and therefore we have considered the parameter $\Delta RMSF_i$ to gain a comparative insight into the flexibility of individual protein residues in the presence and absence of AgNPs.[36] It is defined as

$$\Delta RMSF_i = \frac{RMSF_i^{complex} - RMSF_i^{native}}{RMSF_i^{native}} \quad (1)$$

where $RMSF_i$ is the RMSF of the side chain of the residue *i*, that without NPs is $RMSF_i^{native}$, and that with NPs is $RMSF_i^{complex}$. An increase/decrease in the flexibility of residue *i* is denoted by a positive/negative value of $\Delta RMSF_i$.

5.5. Secondary Structure Analysis of HSA. Here, we have calculated the change in the secondary structural content of the protein in the absence and presence of the NP during the simulation time using the DSSP tool.[66] The secondary structure is plotted in terms of probability values by the residue number of the protein.

DOI: 10.1021/acsomega.9b02340
ACS Omega 2020, 5, 170−178

Apart from the overall secondary structure of the protein, we are interested to see if the NP has any effect on the alteration of the secondary structure at the residue level of the protein. It will help in measuring the structural changes for individual residues.[36] DSSP gives eight different types of secondary structure elements, but HSA has only helix (α, π, and 3_{10}) and loop (turn, coil, and bend types). Two scores are defined, which quantify the secondary structure for residue i: S^i_{helix} and S^i_{loop}. In order to calculate these scores, we need to determine $N_{\text{helix}}/N_{\text{total}}$ and $N_{\text{loop}}/N_{\text{total}}$ wherein N_{helix} and N_{loop} represents the number of frames in which residue i adopts a helix-and-loop type of secondary structure and N_{total} represents the total number of selected frames in the trajectories at regular intervals. $N_{\text{helix}}/N_{\text{total}}$ and $N_{\text{loop}}/N_{\text{total}}$ is equal to S^i_{helix} and S^i_{loop}, respectively, for each residue i. S^i_{helix} and S^i_{loop} measure the frequency of the secondary-structure type (helix and loop) for residue i during the simulation time.[36]

These two scores shall be utilized in the quantification of ΔSec_i. It is the maximum change in the secondary structure of residue i of the HSA when it binds with the AgNP.[36]

$$\Delta\text{Sec}_i = \max|S_i^f(\text{conjugate}) - S_i^f(\text{native})| \quad (2)$$

where f = helix and loop.

Here, S_i^f(conjugate) and S_i^f(native) represent the secondary structure scores of residue i in the conjugate and native structures. ΔSec_i provides two key points of information, that is, the possible change in the secondary structure in the HSA and which among the two secondary structures experiences the alteration: helix or loop.

5.6. Nonbonded Contacts. In order to measure the interaction between the NP and protein, the number of nonbonded contacts was calculated for all the five complexes. It has been reported that the nonbonded contacts exist within the range of 5−7 Å.[67] We have chosen a cutoff of 6 Å to account for any nonbonded interaction between the atoms of the protein and the AgNP. The number of interacting pairs of atoms was defined as the number of contacts between the protein and nanoparticle. The total number of nonbonded contacts changes during the course of simulation, which was used as a parameter to measure the protein−NP interaction. The number of amino acids of the protein, which comes within a radius of 6 Å from the silver nanoparticle atoms, was tracked for all the protein−NP conjugates.

5.7. Protein−AgNP Interaction Energy. In order to quantify the interaction between the protein and AgNP, we have extracted the average energies from all the simulation trajectories of AgNP (E_{np}), protein (E_{protein}), and HSA−AgNP (E_{ORN}) for each of the five conjugates. The total energy of the system comprises the sum of the potential and kinetic energies. The potential energy term contributes toward the bonded and nonbonded interactions within the system. As our system of study entails the protein and AgNP, which are nonbonded in nature, we therefore considered the nonbonded energy component along with the total energy to understand the system's stability. The nonbonded energy is the sum of the van der Waals and Coulombic energies. Herein, three energy terms, which contribute significantly toward the system interaction, were considered: short-range (SR) Coulombic, potential, and total energies. The interaction energy (ΔE) is calculated as the difference in energy of the conjugates (E_{ORN}) and the sum of the energies of the protein (E_{protein}) and AgNP (E_{np}).

$$\Delta E = E_{\text{ORN}} - [E_{\text{protein}} + E_{\text{np}}] \quad (3)$$

where E_{protein} and E_{np} is the average energy of the protein and nanoparticles for their independent simulations. E_{ORN} is the energy of the protein−NP system in the case of MD simulations of conjugated systems. A negative value of ΔE shall indicate a stable serum albumin and silver nanoparticle conjugate.

■ ASSOCIATED CONTENT

Supporting Information

The Supporting Information is available free of charge at https://pubs.acs.org/doi/10.1021/acsomega.9b02340.

Multiple sequence alignment of different types of serum albumin, RMSD plot of the domains oriented toward the NP, secondary structure probability plot, initial orientations of HSA with AgNPs, table representing residues within 6 Å of the NP, and repeat simulations of 100 ns (Figures S5−S7 and Tables S2−S4) (PDF)

■ AUTHOR INFORMATION

Corresponding Author

*E-mail: anjha@tezu.ernet.in. Phone: +91- 3712-275416. Fax: +91-3712-267005.

Author Contributions

Z.H. and A.N.J. performed the interpretation of the data and wrote the manuscript. The entire project was planned and supervised by A.N.J. The authors have read and approved the final manuscript.

Funding

This research did not receive any specific grant from any funding agencies.

Notes

The authors declare no competing financial interest.

■ ACKNOWLEDGMENTS

We acknowledge the Department of Biotechnology (nos. BT/PR15847/NER/95/21/2015 and BT/PR15914/NER/95/33/2015), Government of India, for providing computational facilities and a fellowship to Z.H. Authors acknowledge Dr. Indu Kumari for several discussions, proofreading, and editing.

■ ABBREVIATIONS

HSA: human serum albumin
AgNP: silver nanoparticle
MDS: molecular dynamics simulation

■ REFERENCES

(1) Moriarty, P. Nanostructured materials. *Rep. Prog. Phys.* **2001**, *64*, 297−381.

(2) Neamtu, M.; Nadejde, C.; Hodoroaba, V.-D.; Schneider, R. J.; Verestiuc, L.; Panne, U. Functionalized magnetic nanoparticles: Synthesis, characterization, catalytic application and assessment of toxicity. *Sci. Rep.* **2018**, *8*, 6278.

(3) Tang, X.; Haddad, P.-A.; Mager, N.; Geng, X.; Reckinger, N.; Hermans, S.; Debliquy, M.; Raskin, J.-P. Chemically deposited palladium nanoparticles on graphene for hydrogen sensor applications. *Sci. Rep.* **2019**, *9*, 3653.

(4) Chen, Y. S.; Zhao, Y.; Yoon, S. J.; Gambhir, S. S.; Emelianov, S. Miniature gold nanorods for photoacoustic molecular imaging in the second near-infrared optical window. *Nat. Nanotechnol.* **2019**, *14*, 465−472.

DOI: 10.1021/acsomega.9b02340
ACS Omega 2020, 5, 170−178

(5) Sheehan, S. W.; Noh, H.; Brudvig, G. W.; Cao, H.; Schmuttenmaer, C. A. Plasmonic Enhancement of Dye-Sensitized Solar Cells Using Core−Shell−Shell Nanostructures. *J. Phys. Chem. C* **2013**, *117*, 927−934.
(6) Stark, W. J.; Stoessel, P. R.; Wohlleben, W.; Hafner, A. Industrial applications of nanoparticles. *Chem. Soc. Rev.* **2015**, *44*, 5793−5805.
(7) Cha, B. G.; Kim, J. Functional mesoporous silica nanoparticles for bio-imaging applications. *Wiley Interdiscip. Rev.: Nanomed. Nanobiotechnol.* **2019**, *11*, No. e1515.
(8) Wolfbeis, O. S. An overview of nanoparticles commonly used in fluorescent bioimaging. *Chem. Soc. Rev.* **2015**, *44*, 4743−4768.
(9) Bejarano, J.; Navarro-Marquez, M.; Morales-Zavala, F.; Morales, J. O.; Garcia-Carvajal, I.; Araya-Fuentes, E.; Flores, Y.; Verdejo, H. E.; Castro, P. F.; Lavandero, S.; Kogan, M. J. Nanoparticles for diagnosis and therapy of atherosclerosis and myocardial infarction: evolution toward prospective theranostic approaches. *Theranostics* **2018**, *8*, 4710−4732.
(10) Baetke, S. C.; Lammers, T.; Kiessling, F. Applications of nanoparticles for diagnosis and therapy of cancer. *Br. J. Radiol.* **2015**, *88*, 20150207.
(11) Saraiva, C.; Praça, C.; Ferreira, R.; Santos, T.; Ferreira, L.; Bernardino, L. Nanoparticle-mediated brain drug delivery: Overcoming blood-brain barrier to treat neurodegenerative diseases. *J. Controlled Release* **2016**, *235*, 34−47.
(12) Patra, J. K.; Das, G.; Fraceto, L. F.; Campos, E. V. R.; Rodriguez-Torres, M. D. P.; Acosta-Torres, L. S.; Diaz-Torres, L. A.; Grillo, R.; Swamy, M. K.; Sharma, S.; Habtemariam, S.; Shin, H.-S. Nano based drug delivery systems: recent developments and future prospects. *J. Nanobiotechnol.* **2018**, *16*, 71.
(13) Calzoni, E.; Cesaretti, A.; Polchi, A.; Di Michele, A.; Tancini, B.; Emiliani, C. Biocompatible Polymer Nanoparticles for Drug Delivery Applications in Cancer and Neurodegenerative Disorder Therapies. *J. Funct. Biomater.* **2019**, *10*, 4.
(14) Mu, Q.; Jiang, G.; Chen, L.; Zhou, H.; Fourches, D.; Tropsha, A.; Yan, B. Chemical Basis of Interactions Between Engineered Nanoparticles and Biological Systems. *Chem. Rev.* **2014**, *114*, 7740−7781.
(15) Nayak, P. S.; Borah, S. M.; Gogoi, H.; Asthana, S.; Bhatnagar, R.; Jha, A. N.; Jha, S. Lactoferrin adsorption onto silver nanoparticle interface: Implications of corona on protein conformation, nanoparticle cytotoxicity and the formulation adjuvanticity. *Chem. Eng. J.* **2019**, *361*, 470−484.
(16) Zhang, L.; Feng, M.; Zhou, R.; Luan, B. Structural perturbations on huntingtin N17 domain during its folding on 2D-nanomaterials. *Nanotechnology* **2017**, *28*, 354001.
(17) Ahmed, L.; Rasulev, B.; Kar, S.; Krupa, P.; Mozolewska, M. A.; Leszczynski, J. Inhibitors or toxins? Large library target-specific screening of fullerene-based nanoparticles for drug design purpose. *Nanoscale* **2017**, *9*, 10263−10276.
(18) Chatterjee, T.; Chakraborti, S.; Joshi, P.; Singh, S. P.; Gupta, V.; Chakrabarti, P. The effect of zinc oxide nanoparticles on the structure of the periplasmic domain of the Vibrio cholerae ToxR protein. *FEBS J.* **2010**, *277*, 4184−4194.
(19) Radic, S.; Nedumpully-Govindan, P.; Chen, R.; Salonen, E.; Brown, J. M.; Ke, P. C.; Ding, F. Effect of fullerenol surface chemistry on nanoparticle binding-induced protein misfolding. *Nanoscale* **2014**, *6*, 8340−8349.
(20) Tang, M.; Gandhi, N. S.; Burrage, K.; Gu, Y. Interaction of gold nanosurfaces/nanoparticles with collagen-like peptides. *Phys. Chem. Chem. Phys.* **2019**, *21*, 3701−3711.
(21) Luan, B.; Huynh, T.; Zhao, L.; Zhou, R. Potential Toxicity of Graphene to Cell Functions via Disrupting Protein-Protein Interactions. *ACS Nano* **2015**, *9*, 663−669.
(22) Arakha, M.; Borah, S. M.; Saleem, M.; Jha, A. N.; Jha, S. Interfacial assembly at silver nanoparticle enhances the antibacterial efficacy of nisin. *Free Radicals Biol. Med.* **2016**, *101*, 434−445.
(23) Saikia, N.; Jha, A. N.; Deka, R. C. Dynamics of Fullerene-Mediated Heat-Driven Release of Drug Molecules from Carbon Nanotubes. *J. Phys. Chem. Lett.* **2013**, *4*, 4126−4132.
(24) Saikia, N.; Jha, A. N.; Deka, R. C. Molecular dynamics study on graphene-mediated pyrazinamide drug delivery onto the pncA protein. *RSC Adv.* **2014**, *4*, 24944−24954.
(25) Saikia, N.; Jha, A. N.; Deka, R. C. Interaction of pyrazinamide drug functionalized carbon and boron nitride nanotubes with pncA protein: a molecular dynamics and density functional approach. *RSC Adv.* **2013**, *3*, 15102−15107.
(26) Asthana, S.; Hazarika, Z.; Nayak, P. S.; Roy, J.; Jha, A. N.; Mallick, B.; Jha, S. Insulin adsorption onto zinc oxide nanoparticle mediates conformational rearrangement into amyloid-prone structure with enhanced cytotoxic propensity. *Biochim. Biophys. Acta, Gen. Subj.* **2019**, *1863*, 153−166.
(27) Fanali, G.; Ascenzi, P.; Bernardi, G.; Fasano, M. Sequence analysis of serum albumins reveals the molecular evolution of ligand recognition properties. *J. Biomol. Struct. Dyn.* **2012**, *29*, 691−701.
(28) Li, S.; Cao, Y.; Geng, F. Genome-Wide Identification and Comparative Analysis of Albumin Family in Vertebrates. *Evol. Bioinf. Online* **2017**, *13*, 1176934317716089.
(29) Fanali, G.; di Masi, A.; Trezza, V.; Marino, M.; Fasano, M.; Ascenzi, P. Human serum albumin: from bench to bedside. *Mol. Aspects Med.* **2012**, *33*, 209.
(30) Berman, H. M.; Westbrook, J.; Feng, Z.; Gilliland, G.; Bhat, T. N.; Weissig, H.; Shindyalov, I. N.; Bourne, P. E. The Protein Data Bank. *Nucleic Acids Res.* **2000**, *28*, 235−242.
(31) Yaseen, Z.; Aswal, V. K.; Zhou, X.; Kabir-ud-Din; Haider, S. Morphological changes in human serum albumin in the presence of cationic amphiphilic drugs. *New J. Chem.* **2018**, *42*, 2270−2277.
(32) Zsila, F.; Bikadi, Z.; Malik, D.; Hari, P.; Pechan, I.; Berces, A.; Hazai, E. Evaluation of drug-human serum albumin binding interactions with support vector machine aided online automated docking. *Bioinformatics* **2011**, *27*, 1806−1813.
(33) Tayyab, S.; Izzudin, M. M.; Kabir, Z.; Feroz, S. R.; Tee, W.-V.; Mohamad, S. B.; Alias, Z. Binding of an anticancer drug, axitinib to human serum albumin: Fluorescence quenching and molecular docking study. *J. Photochem. Photobiol., B* **2016**, *162*, 386−394.
(34) Gou, Y.; Zhang, Z.; Li, D.; Zhao, L.; Cai, M.; Sun, Z.; Li, Y.; Zhang, Y.; Khan, H.; Sun, H.; Wang, T.; Liang, H.; Yang, F. HSA-based multi-target combination therapy: regulating drugs' release from HSA and overcoming single drug resistance in a breast cancer model. *Drug Delivery* **2018**, *25*, 321−329.
(35) Ramezani, F.; Amanlou, M.; Rafii-Tabar, H. Gold nanoparticle shape effects on human serum albumin corona interface: a molecular dynamic study. *J. Nanopart. Res.* **2014**, *16*, 2512.
(36) Shao, Q.; Hall, C. K. Allosteric effects of gold nanoparticles on human serum albumin. *Nanoscale* **2017**, *9*, 380−390.
(37) Leonis, G.; Avramopoulos, A.; Papavasileiou, K. D.; Reis, H.; Steinbrecher, T.; Papadopoulos, M. G. A Comprehensive Computational Study of the Interaction between Human Serum Albumin and Fullerenes. *J. Phys. Chem. B* **2015**, *119*, 14971−14985.
(38) López-Esparza, J.; Espinosa-Cristóbal, L. F.; Donohue-Cornejo, A.; Reyes-López, S. Y. Antimicrobial Activity of Silver Nanoparticles in Polycaprolactone Nanofibers against Gram-Positive and Gram-Negative Bacteria. *Ind. Eng. Chem. Res.* **2016**, *55*, 12532−12538.
(39) Sim, W.; Barnard, R. T.; Blaskovich, M. A. T.; Ziora, Z. M. Antimicrobial Silver in Medicinal and Consumer Applications: A Patent Review of the Past Decade (2007(−)2017). *Antibiotics* **2018**, *7*, 93.
(40) Sambale, F.; Wagner, S.; Stahl, F.; Khaydarov, R. R.; Scheper, T.; Bahnemann, D. Investigations of the Toxic Effect of Silver Nanoparticles on Mammalian Cell Lines. *J. Nanomater.* **2015**, 6.
(41) Stensberg, M. C.; Wei, Q.; McLamore, E. S.; Porterfield, D. M.; Wei, A.; Sepúlveda, M. S. Toxicological studies on silver nanoparticles: challenges and opportunities in assessment, monitoring and imaging. *Nanomedicine* **2011**, *6*, 879−898.
(42) Baler, K.; Martin, O. A.; Carignano, M. A.; Ameer, G. A.; Vila, J. A.; Szleifer, I. Electrostatic Unfolding and Interactions of Albumin Driven by pH Changes: A Molecular Dynamics Study. *J. Phys. Chem. B* **2014**, *118*, 921−930.

DOI: 10.1021/acsomega.9b02340
ACS Omega 2020, 5, 170−178

(43) Castellanos, M. M.; Colina, C. M. Molecular Dynamics Simulations of Human Serum Albumin and Role of Disulfide Bonds. *J. Phys. Chem. B* **2013**, *117*, 11895−11905.
(44) Dyawanapelly, S.; Jagtap, D. D.; Dandekar, P.; Ghosh, G.; Jain, R. Assessing safety and protein interactions of surface-modified iron oxide nanoparticles for potential use in biomedical areas. *Colloids Surf., B* **2017**, *154*, 408−420.
(45) Ghosh, G.; Gaikwad, P. S.; Panicker, L.; Nath, B. B.; Mukhopadhyaya, R. Unfolding and inactivation of proteins by counterions in protein-nanoparticles interaction. *Colloids Surf., B* **2016**, *145*, 194−200.
(46) Ding, F.; Radic, S.; Chen, R.; Chen, P.; Geitner, N. K.; Brown, J. M.; Ke, P. C. Direct observation of a single nanoparticle−ubiquitin corona formation. *Nanoscale* **2013**, *5*, 9162−9169.
(47) Satzer, P.; Svec, F.; Sekot, G.; Jungbauer, A. Protein adsorption onto nanoparticles induces conformational changes: Particle size dependency, kinetics, and mechanisms. *Eng. Life Sci.* **2016**, *16*, 238−246.
(48) Sedgwick, P. What are the four phases of clinical research trials? *Br. Med. J.* **2014**, *348*, g3727.
(49) Altschul, S. F.; Gish, W.; Miller, W.; Myers, E. W.; Lipman, D. J. Basic local alignment search tool. *J. Mol. Biol.* **1990**, *215*, 403−410.
(50) The UniProt Consortium. UniProt: a worldwide hub of protein knowledge. *Nucleic Acids Res.* **2019**, *47*, D506−D515.
(51) Chojnacki, S.; Cowley, A.; Lee, J.; Foix, A.; Lopez, R. Programmatic access to bioinformatics tools from EMBL-EBI update: 2017. *Nucleic Acids Res.* **2017**, *45*, W550−W553.
(52) Sekula, B.; Ciesielska, A.; Rytczak, P.; Koziolkiewicz, M.; Bujacz, A. Structural evidence of the species-dependent albumin binding of the modified cyclic phosphatidic acid with cytotoxic properties. *Biosci. Rep.* **2016**, *36*, No. e00338.
(53) Guizado, T. R. C. Analysis of the structure and dynamics of human serum albumin. *J. Mol. Model.* **2014**, *20*, 2450.
(54) Kyrychenko, A.; Korsun, O. M.; Gubin, I. I.; Kovalenko, S. M.; Kalugin, O. N. Atomistic Simulations of Coating of Silver Nanoparticles with Poly(vinylpyrrolidone) Oligomers: Effect of Oligomer Chain Length. *J. Phys. Chem. C* **2015**, *119*, 7888−7899.
(55) Heinz, H.; Vaia, R. A.; Farmer, B. L.; Naik, R. R. Accurate Simulation of Surfaces and Interfaces of Face-Centered Cubic Metals Using 12-6 and 9-6 Lennard-Jones Potentials. *J. Phys. Chem. C* **2008**, *112*, 17281−17290.
(56) Pettersen, E. F.; Goddard, T. D.; Huang, C. C.; Couch, G. S.; Greenblatt, D. M.; Meng, E. C.; Ferrin, T. E. UCSF Chimera–a visualization system for exploratory research and analysis. *J. Comput. Chem.* **2004**, *25*, 1605−1612.
(57) Bora, N.; Jha, A. N. An integrative approach using systems biology, mutational analysis with molecular dynamics simulation to challenge the functionality of a target protein. *Chem. Biol. Drug Des.* **2019**, *93*, 1050−1060.
(58) Das, S.; Khanikar, P.; Hazarika, Z.; Rohman, M. A.; Uzir, A.; Nath Jha, A.; Roy, A. S. Deciphering the Interaction of 5,7-Dihydroxyflavone with Hen-Egg-White Lysozyme through Multi-spectroscopic and Molecular Dynamics Simulation Approaches. *ChemistrySelect* **2018**, *3*, 4911−4922.
(59) Rajkhowa, S.; Jha, A. N.; Deka, R. C. Anti-tubercular drug development: computational strategies to identify potential compounds. *J. Mol. Graphics Modell.* **2015**, *62*, 56−68.
(60) Das, S.; Bora, N.; Rohman, M. A.; Sharma, R.; Jha, A. N.; Roy, A. S. Molecular recognition of bio-active flavonoids quercetin and rutin by bovine hemoglobin: an overview of the binding mechanism, thermodynamics and structural aspects through multi-spectroscopic and molecular dynamics simulation studies. *Phys. Chem. Chem. Phys.* **2018**, *20*, 21668−21684.
(61) Van Der Spoel, D.; Lindahl, E.; Hess, B.; Groenhof, G.; Mark, A. E.; Berendsen, H. J. C. GROMACS: fast, flexible, and free. *J. Comput. Chem.* **2005**, *26*, 1701−1718.
(62) Abraham, M. J.; Murtola, T.; Schulz, R.; Páll, S.; Smith, J. C.; Hess, B.; Lindahl, E. GROMACS: High performance molecular simulations through multi-level parallelism from laptops to supercomputers. *SoftwareX* **2015**, *1-2*, 19−25.
(63) Hess, B.; Bekker, H.; Berendsen, H. J. C.; Fraaije, J. G. E. M. LINCS: A linear constraint solver for molecular simulations. *J. Comput. Chem.* **1997**, *18*, 1463−1472.
(64) Bussi, G.; Donadio, D.; Parrinello, M. Canonical sampling through velocity rescaling. *J. Chem. Phys.* **2007**, *126*, 014101−014107.
(65) Parrinello, M.; Rahman, A. Polymorphic transitions in single crystals: A new molecular dynamics method. *J. Appl. Phys.* **1981**, *52*, 7182−7190.
(66) Kabsch, W.; Sander, C. Dictionary of protein secondary structure: pattern recognition of hydrogen-bonded and geometrical features. *Biopolymers* **1983**, *22*, 2577−2637.
(67) Jha, A. N.; Vishveshwara, S.; Banavar, J. R. Amino acid interaction preferences in proteins. *Protein Sci.* **2010**, *19*, 603−616.

DOI: 10.1021/acsomega.9b02340
ACS Omega 2020, 5, 170−178